*Superlattices and Microstructures, Vol. 26, No. 3, 1999*
Article No. spmi.1999.0778
Available online at http://www.idealibrary.com on IDEAL

# Infrared spectroscopy of intraband transitions in Ge/Si quantum dot superlattices

WEN-GANG WU, JIAN-LIN LIU, YIN-SHENG TANG, KANG L. WANG
*Device Research Laboratory, Department of Electrical Engineering, University of California, Los Angeles, CA 90095-1594, U.S.A.*

*(Received 23 July 1999)*

We report the study of infrared spectroscopy of intraband transitions in Ge/Si quantum dot superlattices. The superlattices, which were grown on (001) oriented Si substrates by a solid source molecular beam epitaxy system, are composed mainly of 20 or 30 periods of Ge dot layers and Si spacer films. The structural properties of them and of the uncapped Ge dots grown on the surfaces of some of them were tested by cross-sectional transmission electron and atomic force microscopes, respectively. It is found that the Ge quantum dots have flat lens-like shapes. Infrared absorption signals peaking in the mid-infrared range were observed using Fourier transform infrared and Raman scattering spectroscopy techniques. Experimental and theoretical analysis suggests that the mid-infrared response be attributed to intraband transitions within the valence band of the Ge quantum dots in the superlattices. The fact that the intraband absorption is strongly polarized along the growth axis of the superlattices signifies that the Ge quantum dots with flat lens-like shapes perform as Ge/Si-based quantum wells. This study demonstrates the application potential of these kinds of Ge/Si quantum dot superlattices for developing mid-infrared photodetectors.



**Key words:** Ge quantum dot, intraband transition, infrared, superlattice.

## 1. Introduction

Self-assembled quantum dots (QDs) remain a topic of great fundamental and technological interest in their optical properties due to intraband transitions over the past few years. This interest is primarily stimulated by the anticipation that the success achieved in using quantum well structures in novel infrared photodetectors and imaging focal plane arrays would be able to be extended to using QDs in these devices. For this application, one of the advantages of quasi-zero-dimensional QDs as compared with quantum wells (QWs) is their intrinsic ability to absorb normal-incidence radiation [1, 2]. Furthermore, the predicted slowing of the intraband relaxation process [3–5] due to reduced carrier–phonon interaction [6] could help detector performance. Owing to the low and sharp $\delta$-like density of states of QDs, the dark current levels of quantum dot infrared photodetectors (ODIPs) are expected to be low when an appropriate doping concentration is selected. To date, most of the reported works about optical properties due to intraband transitions in QDs were done on III–V-based quantum dot structures using a variety of spectroscopy techniques. Drexler *et al*. [7] investigated the intraband absorption of charged InGaAs QDs using a capacitance spectroscopy technique coupled with

0749–6036/99/090219 + 09 $30.00/0 

a far-infrared spectrometer. Phillips *et al*. [8] studied the far-infrared absorption of Si-doped InAs QDs with GaAs and $Al_{0.15}Ga_{0.85}As$ as the barrier materials in the range $10 \sim 20$ $\mu$m using a Fourier transform infrared (FTIR) spectrometer. Sauvage *et al*. [9, 10] made researches on the intraband absorption of undoped and doped InAs using photoinduced infrared absorption and FTIR techniques. Berryman *et al*. [11] observed the mid-infrared intraband absorption in self-organized InAs/$In_xGa_{1-x}As$ clusters using mid-infrared photoconductivity measurements. Recently, normal incidence infrared absorption in an InGaAs/GaAs quantum dot superlattice and the polarization dependence of the intraband absorption in *n*-doped InAs and InGaAs QDs embedded in a GaAs matrix have been reported [1, 2, 12]. However, very limited work has been done on the intraband absorption features of Ge/Si quantum dot structures. In fact, a large valence band offset in quasi-zero-dimensional Ge/Si heterojunction system as well as a small hole effective mass favors hole intraband transitions for near-far- or mid-infrared applications [13]. Another key advantage of using epitaxial Ge/Si quantum dot structures for fabricating infrared detectors is that the monolithic integration with the mature Si-processing-based signal electronics can be achieved. With the recent success in producing high-quality, controllable Ge QDs on Si matrix [14–16] by the rediscovered Stranski–Krastanow growth mode [17, 18] in molecular beam epitaxy (MBE), it is timely to examine the optical nature of the intraband transitions in Ge/Si quantum dot structures. In this paper, we report the investigation of the mid-infrared intraband absorption and its polarization dependence in Ge/Si quantum dot superlattice with boron-doped or modulation boron-doped Ge QDs using FTIR and Raman scattering spectroscopy techniques.

## 2. Sample growth and test

Two kinds of Ge/Si quantum dot superlattices, grown by a solid-source MBE system on (001) oriented Si substrates with the resistivity of $18 \sim 25$ $\Omega$ cm, were investigated in our experiments. For the first one, from the substrate up, a typical structure consists of a 200 nm undoped Si buffer layer and a 20 period Ge/Si quantum dot multilayers, each with a thin heavily boron-doped self-organized Ge dot layer sandwiched in between two 6 nm undoped Si spacer films. The structure of the second one is composed mainly of 30 layers of undoped self-assembled Ge QDs. The Ge dot layers are separated with boron-doped Si spacers. The thickness of the Si spacer films in this kind of superlattice is also about 6 nm each. Figure 1 demonstrates the schematic of MBE growth structure of the Ge/Si quantum dot superlattices. These quantum dot superlattices were grown epitaxially at a substrate temperature of 650°C. The nominal growth rates are 1 and 0.2 Å $s^{-1}$ for Si and Ge, respectively. Boron doping was achieved by thermal evaporation. Before the growth, the substrates were cleaned by the standard Shiraki's cleaning procedure and then introduced into the MBE system immediately. The protective oxide layers covering the surfaces of the Si substrates were removed subsequently by heating the substrates to 930°C for 15 min.

The samples were examined with cross-sectional transmission electron microscopy (TEM), which indicated evidence of the existence of the Ge/Si quantum dot superlattice structures. Figure 2 shows the cross-sectional TEM image of the first kind of superlattice. No misfit dislocations are observed within the whole TEM image area. The area densities of the boron-doped and modulation boron-doped Ge QDs are around $2 \times 10^8$ and $5 \times 10^9$ $cm^{-2}$, respectively. These numbers are determined by atomic force microscopy (AFM) measurements performed on corresponding reference Ge/Si quantum dot superlattice samples grown under the same growth conditions, but without the top Si cap layers. Because of the small spacing between the dot layers the Ge QDs are possible very much to be stacked on top of each other along the growth direction while their in-plane positions are random. Therefore, it can be estimated that the concentration of the dots per layer is constant and the periodicity of the structure along the growth direction is excellent. AFM measurements also demonstrate that the Ge QDs have flat lens-like shapes. The typical base dimension and height of the boron-doped or modulation boron-doped Ge dots in the array are 42 and 4 nm or 38 and $3 \sim 4$ nm, respectively, which are consistent with the data obtained from TEM measurements. The nonuniformity of

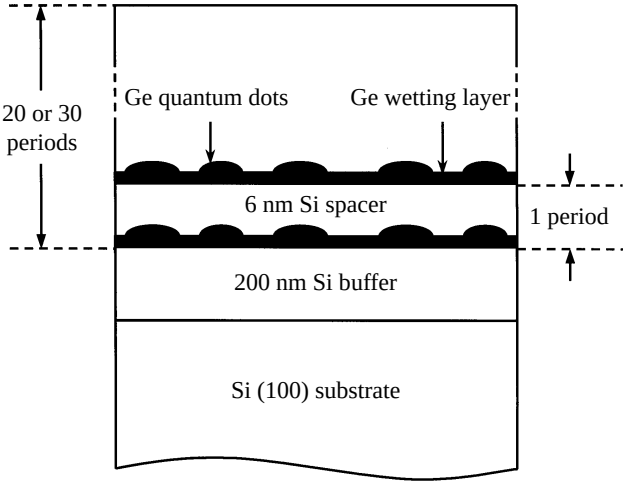


**Fig. 1.** Schematic of MBE growth structure of Ge/Si quantum dot superlattice with boron-doped or modulation boron-doped Ge QDs.

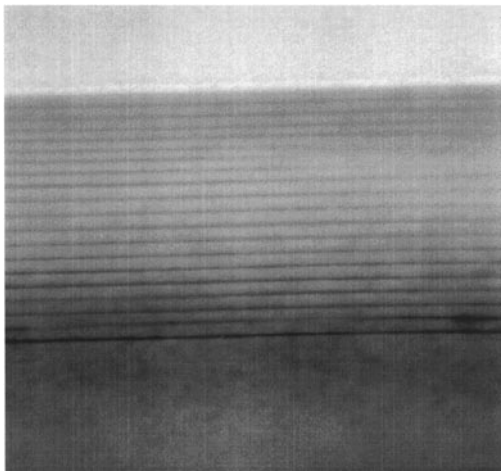

**Fig. 2.** Cross-sectional TEM image of the Ge/Si quantum dot superlattice with directly boron-doped Ge QDs. Twenty periods of flat lens-like Ge dot layers (thin and black) and Si spacer films (thick and white) can be seen clearly.

the dot size is estimated to be $\pm 10\%$. Figure 3 shows the AFM image and shape profile of the modulation boron-doped Ge QDs.

## 3. Experiments and discussion

For FTIR measurements, the Ge/Si quantum dot superlattice samples were produced into multi-reflection waveguides of 10 mm $\times$ 5 mm in size and with polished 45° facets and backside in order to increase net absorption, as shown schematically in the inset of the Fig. 4. A beam condenser was used to focus the incoming infrared beam onto the waveguides. The polarization of the incidence infrared beam was set by an infrared polarizer, which was placed in the light path, so that the polarization dependence features of the infrared absorption could be probed. A Si (100) substrate waveguide with the same dimension was used as

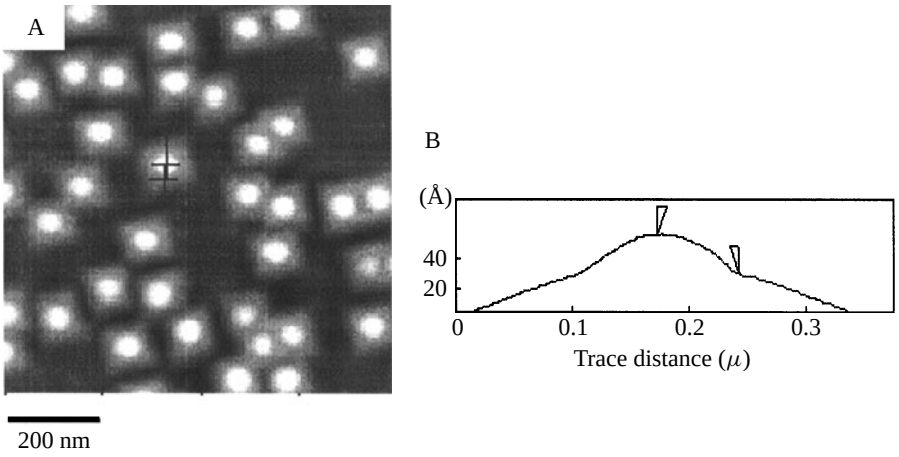


**Fig. 3.** A, AFM image of the modulation boron-doped Ge QDs grown on the surface of the second kind of superlattice, and B, AFM shape profile of one of the dots.

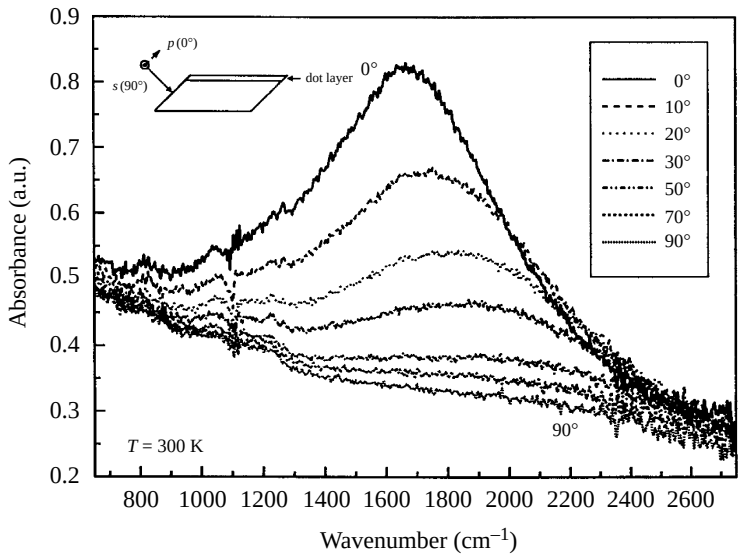


**Fig. 4.** Room temperature infrared absorption spectra of the directly boron-doped flat lens-like Ge QDs under different polarization directions of the incidence light. The inset shows a waveguide structure and how the p- and s-polarization of the incidence light is defined.

the correspondent reference sample. The measurements were performed at room temperature with a Nicolet FTIR spectrometer.

The measured infrared absorption spectra of the Ge/Si quantum dot superlattices with boron-doped and modulation boron-doped Ge QDs are shown in Figs 4 and 5, respectively. A strong polarization dependence feature in the spectra is observed. Under 0° polarization (p-polarization), broad absorption peaks with the strongest intensities are observed around 1683 and 2004 cm$^{-1}$ for the superlattices with boron-doped and modulation boron-doped Ge dots, respectively. As the polarization angle of the incidence infrared light in-

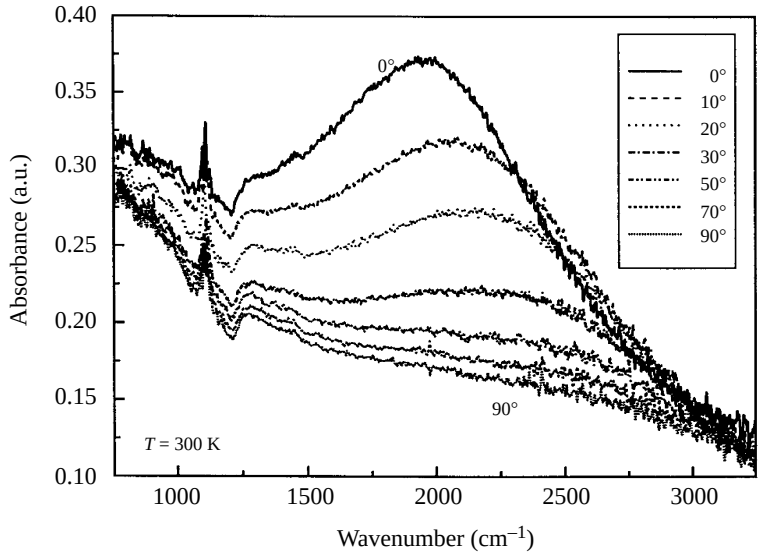


**Fig. 5.** Room temperature infrared absorption spectra of the modulation boron-doped flat lens-like Ge QDs under different polarization directions of the incidence light.

creases, the absorption peak intensities decrease until no clear absorption can be seen in the infrared spectral range investigated under 90° polarization (s-polarization), except for the free carrier background absorption.

It should be noted that the positions of the above-observed infrared absorption peaks of the Ge/Si quantum dot superlattices are comparable to the energy separation between the lowest and the second states in the valence band of the flat lens-like Ge QDs in the superlattices, which is determined by theoretical calculation. For simply, a lens-like Ge quantum dot can be treated as an infinite-barrier quantum box but no exciton effects as well as dielectric screening [13, 19, 20] are considered. Thus, the energies of the allowed hole states in the dot can be evaluated precisely as follows:

$$E_{n,k,l} = \frac{\pi^2\hbar^2}{2m^*}\left(\frac{n^2}{L_x^2} + \frac{k^2}{L_y^2} + \frac{l^2}{L_z^2}\right), \qquad n, k, l = 1, 2, 3, \ldots \tag{1}$$

where $m^*$ represents Ge hole effective mass, $L_x$ and $L_y$ are the base dimensions of the dot while $L_z$ is its height. In calculation, the effective masses of $0.32m_0$ and $0.044m_0$ for heavy and light holes, respectively, and the typical values of the base dimension and height of the actual flat lens-like Ge QDs, which are obtained from AFM and TEM measurements, are used. Under this condition, the first two terms in eqn (1) can be omitted because both $L_x$ and $L_y$ (42 or 38 nm) are much larger than $L_z$ (4 or $3 \sim 4$ nm). With regard to the directly boron-doped Ge QDs, the calculation demonstrates that, in the valence band, the first two heavy hole levels locate at 73 and 292 meV, respectively, while the energy of the first light hole state is about 530 meV. As known, the possible largest barrier for both heavy and light holes in the dots is the bandgap difference between Si and Ge ($1.12 - 0.67$ eV $= 0.45$ eV)[†]if we assume that this band offset is consumed entirely in the valence band. Therefore, it can be easily understood that there are no confined light hole states in the dots themselves because of the small dot size and small light hole effective mass as well, while there exist at least two heavy hole bound states in the dots. The light hole levels, which are in fact the virtual continua below the valence band edge of the Si barrier, should not be occupied. It is found that the calculated energy separation between

[†]This number is estimated based on unstrained Ge dots and underlying Si. The presence of strain will change the bandgaps of Si and Ge, and thus the corresponding band offset.

the ground and the first excited heavy hole states is 219 meV and closed to the measured absorption peak energy of 209 meV ($\sim 6\ \mu$m) for 0° polarization for the superlattice with the directly boron-doped Ge dots. The little difference between the experimental and theoretical data may be due to the fact that the coupling among the corresponding heavy hole quasi-bound states in different Ge dots along the growth direction is not taken into the calculation account. As mentioned above, thin spacing between the Ge dot layers makes the Ge QDs have the tendency of being stacked on top of each other along the growth direction. Thus, in the direction, it is possible very much that the corresponding heavy hole quasi-bound states in different Ge dots couple together to form superlattice minibands [21]. Actually, the energy separation between the first two heavy hole minibands in the Ge/Si quantum dot superlattice is slightly smaller than that between the first two heavy hole bound states in just one Ge quantum dot. With regard to the modulation boron-doped Ge QDs, the calculated energy separation between the ground and the first excited heavy hole states is about 270 meV while, for 0° polarization, the absorption peak energy of the superlattice with the modulation boron-doped Ge dots is measured at 248 meV ($\sim 5\ \mu$m). Besides the formation of heavy hole minibands along the growth direction of the superlattice, band bending due to the space separation between donors and holes, and valence band mixing, etc. may have a certain contribution to the larger difference between the theoretical and experimental data. According to the above analysis, we attribute the infrared absorption observed to the intraband transition within the valence band of the flat lens-like Ge QDs.

As shown in Figs 4 and 5, for 0° polarization, the full widths at half maximum (FWHM) of the intraband absorption peaks are about 75 and 96 meV for the superlattices with boron-doped and modulation boron-doped Ge dots, respectively. The size distribution of the self-organized Ge QDs is the main contribution to the large broadening of the absorption peaks. The nonparabolicity of the hole bands may also play a strong role in this case as was observed in the quantum well case [13, 19, 22].

In Figs 4 and 5, absorption signals, which are believed to result from the Ge wetting layers, are found to locate at 1230 and 1280 $cm^{-1}$ for the superlattices with boron-doped and modulation boron-doped Ge dots, respectively. It can be judged that the wetting layers in these two kinds of superlattices are about the same under almost the same growth conditions (for example, growth temperature) [23]. In addition, a sharp peak near 1100 $cm^{-1}$ is mainly due to the strong infrared absorption from $SiO_2$ and water in the spectral range of interest.

Figure 6 depicts the normalized intraband absorbance versus the polarization angle $\theta$ of the incidence infrared light. The $\cos^2\theta$-like solid line presents the well-known polarization dependence feature of the intersubband transitions in Ge/Si-based QWs grown on Si (100) substrate. The solid square (A) and open triangle (B) symbols are the polarization-dependent data of the normalized intraband absorbance of the Ge/Si quantum dot superlattices with boron-doped and modulation boron-doped Ge QDs, respectively. It can be seen clearly that the intraband absorption intensity decreases with the increasing of the polarization angle $\theta$, the same as what Figs 4 and 5 demonstrate, and the curves have the quantum-well-like feature. A similar quantum-well-like polarization dependence feature about the intraband absorption in *n*-doped InAs/GaAs and InGaAs/GaAs quantum dot systems was reported [10, 12]. Theoretically there should still be obvious intraband absorption under 90° polarization of the incidence infrared light, not as shown in Figs 4–6, because the intraband transitions in quantum dots are also sensitive to normal incidence photoexcitation. However, in the superlattices, the Ge dots sandwiched in between two Si spacer films are usually flattened under most growth conditions [24]. Thus, the dots have relatively large base dimensions while their heights are very small. Accordingly, the quantum confinement becomes strong along the growth direction but weak in the lateral directions. Therefore, the polarization dependence of the intraband absorption in the flat lens-like Ge QDs appears similar to that in the Ge/Si-based QWs.

The intraband absorption within the valence band of the flat lens-like Ge QDs was also investigated using a Raman scattering spectroscopy technique because Raman scattering light that covers almost the whole frequency domain can arouse intraband transitions. The investigation was performed with a Renishaw 2000 Raman spectrometer at room temperature. Raman scattering spectra were excited by the 514 nm line of an

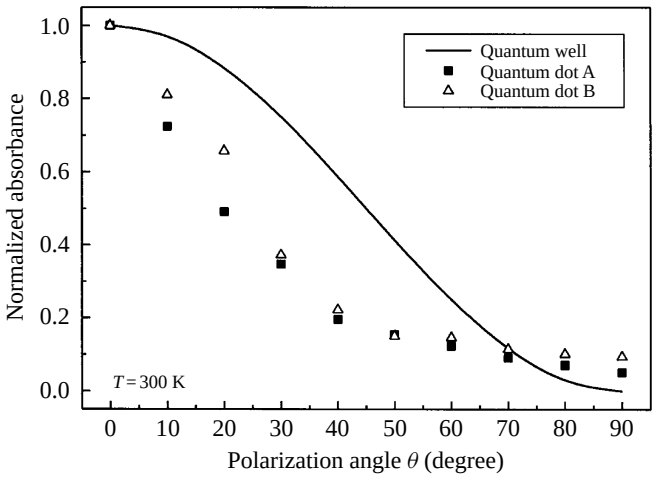


**Fig. 6.** Incidence light polarization angle dependence of the normalized intraband absorbance for boron-doped A, and modulation boron-doped B, Ge QDs. The experimental curves have the quantum-well-like feature.

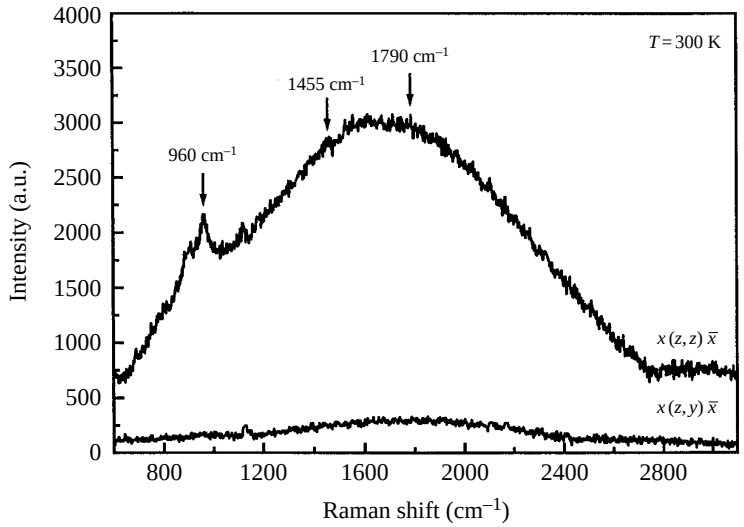


**Fig. 7.** Polarized $(x(z, z)\overline{x})$ and depolarized $(x(z, y)\overline{x})$ Raman spectra of a Ge/Si quantum dot superlattice with directly boron-doped Ge QDs. The arrows at about 1790, 960 and 1455 $cm^{-1}$ indicate the intraband absorption in the flat lens-like Ge dots, the second- and third-order Si optical phonons, respectively.

Ar ion laser in the back-scattering configuration and then recorded by a Si charge couple device (CCD) camera. Figure 7 shows the measured polarization-dependent Raman spectra of another sample of the Ge/Si quantum dot superlattice with directly boron-doped Ge QDs. In the measurement, the incident laser was focused on a cleaved edge side of the sample and the scattering light with polarization in either parallel to the growth direction $(z)$ (so-called polarized spectrum $(x(z, z)\overline{x})$) or perpendicular to the growth direction $(y)$ (so-called depolarized spectrum $(x(z, y)\overline{x})$) was collected. In the polarized Raman spectrum $(x(z, z)\overline{x})$, the broad peak around 1790 $cm^{-1}$ is believed to result from the intraband absorption within the valence band of the Ge dots because its peak energy is in agreement with the calculated energy separation between the first

two heavy hole bound states in a typical flat lens-like dot in the light of the previous theoretical method. Its FWHM is about 100 meV which is close to that observed by FTIR too. The other two peaks at about 960 and 1455 $cm^{-1}$ are attributed to the second- and third-order Si optical phonons. In the depolarized Raman spectrum $(x(z, y)\overline{x})$, the intraband absorption signal is absence in the observed wavenumber range because the Raman tensor should be zero in this configuration according to the selection rules [25, 26]. Meanwhile, there are no clear phonon peaks since the Si optical phonons are forbidden in principle in this case.

## 4. Conclusion

In conclusion, mid-infrared absorption in Ge/Si quantum dot superlattices grown on Si (100) substrates was observed using FTIR and Raman scattering spectroscopy techniques. The absorption is attributed to heavy hole quasi-bound to quasi-bound intraband transition in the flat lens-like Ge QDs in the superlattices and strongly polarized along the growth axis of the structures in the spectral range investigated. The decreasing of the absorption intensity with the increasing of the polarization angle of the incoming infrared light implies that the polarization selection rule of the intraband transitions within the valence band of the flat lens-like Ge QDs is similar to the polarization selection rule of intersubband transitions in the valence band of Ge/Si-based QWs. The successful observation of the mid-infrared intraband absorption in the well-grown Ge/Si quantum dot superlattices provides an impetus to using Ge/Si quantum dot structures to develop mid-infrared photodetectors.

*Acknowledgements*—The work was supported partly by the ARO (DAAG55-98-1-0358), Low Power MURI (DAAH049610005) and National Science Foundation (DMR-9520893).

## References

[1] D. Pan, Y. P. Zeng, M. Y. Kong, J. Wu, Y. Q. Zhu, C. H. Zheng, J. M. Li, and C. Y. Wang, Electron. Lett. **32**, 1726 (1996).
[2] J. C. Phillips, K. Kamath, and P. Bhattacharya, Appl. Phys. Lett. **71**, 2020 (1998).
[3] H. Benisty, C. M. Sottomayor-Torres, and C. Weisbuch, Phys. Rev. **B44**, 10945 (1991).
[4] U. Bockelmenn and G. Bastard, Phys. Rev. **B42**, 8947 (1990).
[5] M. Sugawara, K. Mukai, and H. Shoji, Appl. Phys. Lett. **71**, 2791 (1997).
[6] J. Singh, IEEE Photonics Technol. Lett. **8**, 488 (1996).
[7] H. Drexler, D. Leonard, W. Hansen, J. P. Kotthaus, and P. M. Petroff, Phys. Rev. Lett. **73**, 2252 (1994).
[8] J. Phillips, K. Kamath, X. Zhou, N. Chervela, and P. Bhattacharya, Appl. Phys. Lett. **71**, 2079 (1994).
[9] S. Sauvage, P. Boucaud, F. H. Julien, J.-M. Gerard, and J.-Y. Marzin, J. Appl. Phys. **82**, 3396 (1997).
[10] S. Sauvage, P. Boucaud, F. H. Julien, J.-M. Gerard, and V. Thierry-Mieg, Appl. Phys. Lett. **71**, 2785 (1997).
[11] K. W. Berryman, S. A. Lyon, and M. Segev, Appl. Phys. Lett. **70**, 1861 (1997).
[12] S. J. Chua, S. J. Xu, X. H. Zhang, X. C. Wang, T. Mei, W. J. Fan, C. H. Wang, J. Jiang, and X. G. Xie, Appl. Phys. Lett. **73**, 1997 (1998).
[13] K. L. Wang and R. P. G. Karunasiri, Infrared detectors using SiGe/Si quantum well structures, in *Semiconductor Quantum Wells and Superlattices for Long-wavelength Infrared Detectors*, edited by M. O. Manasreh (Artech House, Boston, 1993).
[14] E. Palange, G. Capellini, L. Di Gaspare, and F. Evangelisti, Appl. Phys. Lett. **68**, 2982 (1996).
[15] S. K. Zhang, H. J. Zhu, F. Lu, Z. M. Jiang, and X. Wang, Phys. Rev. Lett. **80**, 3340 (1998).
[16] J. Tersoff, C. Teichert, and M. G. Lagally, Phys. Rev. Lett. **76**, 1675 (1996).
[17] I. N. Stranski and L. Krastanow, Sitzungsber. Akad. Wiss. Wien Math. Naturwiss. K1 Abt. 2B Chemie **146**, 797 (1937).

[18] D. Leonard, M. Krishnamurthy, C. M. Reaves, S. P. Denbars, and P. M. Petroff, Appl. Phys. Lett. **63**, 3203 (1993).
[19] S. K. Chum, D. S. Pan, and K. L. Wang, Phys. Rev. **B47**, 15638 (1993).
[20] R. P. G. Karunasiri, J. S. Park, and K. L. Wang, Appl. Phys. Lett. **59**, 2588 (1991).
[21] Ting Mei, G. Karunasiri, and S. J. Chua, Appl. Phys. Lett. **71**, 2017 (1997).
[22] P. Kruck, M. Helm, T. Fromherz, G. Bauer, J. F. Nutzel, and G. Abstreiter, Appl. Phys. Lett. **69**, 3372 (1996).
[23] H. Sunamara, S. Fukatsu, N. Usami, and Y. Shiraki, J. Crystal Growth **157**, 265 (1995).
[24] S. Schierker, O. G. Schmidt, K. Eberl, N. Y. Jin-Phillipp, and F. Phillipp, Appl. Phys. Lett. **72**, 3344 (1998).
[25] Y. B. Li, R. A. Stradling, L. Artus, S. J. Webb, R. Cusco, S. J. Chung, and A. G. Norman, Semicond. Sci. Technol. **11**, 1137 (1996).
[26] M. Bendayan, R. Beserman, and K. Dettmer, J. Appl. Phys. **81**, 7956 (1990).